

Rotation-aligned coupling in ^{61}Fe

N. Hoteling,^{1,2} W. B. Walters,¹ R. V. F. Janssens,² R. Broda,³ M. P. Carpenter,² B. Fornal,³ A. A. Hecht,^{1,2} M. Hjorth-Jensen,⁴ W. Królas,^{3,5} T. Lauritsen,² T. Pawłat,³ D. Seweryniak,² J. R. Stone,^{1,6} X. Wang,^{2,7} A. Wöhr,⁷ J. Wrzesiński,³ and S. Zhu²

¹*Department of Chemistry and Biochemistry, University of Maryland, College Park, Maryland 20742, USA*

²*Physics Division, Argonne National Laboratory, Argonne, Illinois 60439, USA*

³*Niewodniczański Institute of Nuclear Physics, Krakow, PL-31342, Poland*

⁴*Department of Physics and Center of Mathematics for Applications, University of Oslo, N-0316 Oslo, Norway*

⁵*Joint Institute for Heavy Ion Research, Oak Ridge, Tennessee 37831, USA*

⁶*Department of Physics, University of Oxford, OX1 3PU Oxford, United Kingdom*

⁷*Department of Physics, University of Notre Dame, Notre Dame, Indiana 46556, USA*

(Received 19 November 2007; published 29 April 2008)

New levels have been established above the 861-keV, $9/2^+$ isomeric state in ^{61}Fe . The observations can be reproduced satisfactorily by shell model calculations, but only after a significant lowering of the $\nu g_{9/2}$ single-particle energy with respect to the value determined empirically from levels outside a ^{48}Ca core. The results are also described well within the scope of the particle-triaxial-rotor model assuming a deformation $\beta_2 \sim 0.24$. The present findings, together with the recently measured magnetic and quadrupole moments of this state, point toward a structure possibly associated with a prolate shape.

DOI: [10.1103/PhysRevC.77.044314](https://doi.org/10.1103/PhysRevC.77.044314)

PACS number(s): 21.10.-k, 23.20.Lv, 27.50.+e

I. INTRODUCTION

Nuclear structure in the vicinity of closed shells often supports the formation of isomeric states. The region around double-magic $^{68}\text{Ni}_{40}$ is no exception, as has been well documented by Grzywacz *et al.* [1]. Although recent studies have demonstrated that the subshell gap at $N = 40$ dissipates below $Z = 28$ [2,3], the emergence of isomeric states still abounds, as in the case of ^{61}Fe , where a $239(5)\text{-ns}$, $9/2^+$ isomer has been investigated in terms of both its magnetic and quadrupole moments [4,5]. As such, it is clear that the disappearance of the $N = 40$ subshell gap arises from an intrusion of the $g_{9/2}$ neutron orbital into the pf shell. This feature is also readily apparent from the systematic trends of $9/2^+$ states in the odd- A Fe and Cr nuclei with respect to Ni, and from the 2^+ energy trends in the corresponding even-even isotopes.

The challenge set forth by such information is whether these observations can be adequately described by current models. For instance, shell model calculations for pf -shell nuclei have typically operated within a strict pf configuration space, with the inherent assumption of an $N = 40$ closed shell [6]. This is clearly not the case, a fact that is emphasized by the inadequacy of such model spaces to describe nuclei in which this subshell is nearly filled. For example, Sorlin *et al.* [3] demonstrated the importance of larger model spaces for the description of the 2^+ energy trends in the Cr isotopes, and Caurier *et al.* [7] reached similar conclusions for the Fe nuclei. In both cases, a larger model space, which included at least the $g_{9/2}$ neutron orbital in addition to the pf orbitals, achieved a much greater degree of success in reproducing the data.

Beyond the pursuit of an adequate shell model description lies the question of whether the increasing significance of the $\nu g_{9/2}$ orbital is the result of an onset of deformation. In fact, a propensity toward deformation was first invoked by Hannawald *et al.* [2] in order to account for the drop

in 2^+ energy observed for $^{64,66}\text{Fe}$, and this suggestion was reiterated by Sorlin *et al.* [3] when they reported a similar trend in the Cr isotopes. However, the level sequences above the 2^+ states do not appear to support this contention [8,9], as noncollective structures are observed in these systems which have been reasonably well described by the shell model, albeit with significant room for improvement. Furthermore, trends in the $E(4_1^+/2_1^+)$ energy ratios in Fe and Cr isotopes do not appear to approach the rotational limit of 3.33 expected for prolate-deformed rotors; rather, these ratios appear to be dropping with increasing neutron number, indicating that another explanation is needed to better account for the structural aspects of this region.

One way to assess the effect of a possible intrusion by the $\nu g_{9/2}$ orbital into the pf shell is to study the intrinsic structure associated with sequences of levels built on top of these $9/2^+$ states in the odd- A isotopes below $Z = 28$. A better understanding of the properties of these $9/2^+$ levels will, in turn, lead to a better understanding of their impact on the respective even-even cores. Recently, investigations of such states in the Cr isotopes have addressed this question. Band structures with regular energy spacings suggestive of collective rotation were reported in $^{55,57}\text{Cr}$ and successful comparisons with total Routhian surface (TRS) calculations suggested a prolate rotational character [10]. The same theoretical approach has been used to suggest a possible transition to a shape with small oblate deformation for the $g_{9/2}$ structure in ^{59}Cr [11]. In ^{61}Fe , a recent measurement of the quadrupole moment of the 861-keV, $9/2^+$ isomeric state [5] implied a deformation $\beta_2 \approx +0.24$ or -0.21 , which the authors used to emphasize the need for more data pertaining to the levels above this isomer, as these could be used to discriminate between possible prolate and oblate deformations.

In this paper, new levels above the $9/2^+$ isomeric state in ^{61}Fe are identified from a measurement using deep inelastic

reactions together with the Gammasphere spectrometer. The observed level sequence can be satisfactorily described in terms of the nuclear shell model, provided that the $\nu g_{9/2}$ orbital is included in the model space with a single-particle energy significantly lower than anticipated. Stimulated by the shape-driving properties of this $g_{9/2}$ neutron orbital, the results were interpreted further in terms of the particle-triaxial-rotor model, which reproduces the data quite well and points toward an interpretation in terms of rotational alignment coupled to a prolate core.

II. EXPERIMENT

The production and subsequent investigation of neutron-rich nuclei in the region around $N = 40$ can pose significant challenges. Most modern techniques still require the use of stable beam-target combinations or, otherwise, do not yet have sufficient resolving power to permit the analysis of prompt deexcitations. In light of this situation, the technique of deep-inelastic reactions has seen considerable use in recent years, especially in the region of interest for this experiment (for a recent review, see Ref. [12]). The recognition that beam-target combinations with maximal composite N/Z ratios tend to produce the most neutron-rich nuclei has served as a general guide for these measurements. Thus, in the experiment reported here, the most neutron-rich stable isotope of Ni, ^{64}Ni , was paired with a thick, 55 mg/cm^2 , ^{238}U target. Ideally, a beam energy roughly 10–20% above the Coulomb barrier is desired, but in an experiment such as this, where product nuclides must be stopped within the target, a higher energy will typically be employed so that the desired reactions occur near the middle of the target. Hence, a beam energy of 430 MeV was chosen, roughly 25% above the Coulomb barrier. The experiment was carried out with the Argonne Tandem Linear Accelerator System (ATLAS) at Argonne National Laboratory. Results for the ^{64}Fe nucleus obtained from this measurement were reported previously in Ref. [9].

Multifold γ -ray coincidence events were recorded with the Gammasphere spectrometer [13], in which 100 Compton-suppressed high-purity Ge detectors surrounded the target chamber centered in the array. A requirement of three-fold coincidence events or higher was employed for most of the experiment, although some data were also collected under a two-fold condition. Events were sorted into four coincidence cubes: prompt-prompt-prompt (PPP), delayed-delayed-delayed (DDD), prompt-prompt-delayed (PPD), and prompt-delayed-delayed (PDD). In this way, the measured time with respect to the beam bursts could be exploited in order to identify transitions associated with short-lived isomers. Specifically, the beam bursts were separated by 410-ns time intervals. Events were considered to be prompt if the detectors fired within ± 20 ns of a beam burst, and delayed if they were detected within ~ 800 ns of a particular burst (excluding events that came during the next burst). The probability for contamination of delayed coincidences arising from subsequent beam bursts was small owing to the reaction cross section for beam and target. According to the data, the counts in the burst immediately following an event were approximately two orders of magnitude smaller than those

recorded during the prompt burst, and therefore the probability for contamination of delayed spectra was negligibly small. Data were collected for approximately 5 days with an average beam intensity of $\sim 4 \times 10^8$ ions per second.

Coincidence events can also be analyzed with respect to the angle between the detectors that fired. Each γ ray can be considered aligned with respect to its coincidence partner, and multipolarities can be deduced on the basis of an angular correlation analysis, as described in Ref. [9].

III. RESULTS

The structure of ^{61}Fe was previously investigated using β -decay [14], fragmentation [1], and, to some extent, deep-inelastic [15] reactions. From these studies, a 239(5)-ns isomeric state was established at 861 keV [1,16]. This state has been determined to represent the $9/2^+$ level associated with the occupation of the $g_{9/2}$ neutron orbital by a single neutron [4]. Above this isomer, a γ ray at 789 keV has been reported, deduced from the prompt-delayed coincidence matrix obtained in a deep-inelastic reaction with ^{64}Ni and ^{130}Te [15]. In the present study, triple-coincidence data are used to establish several new transitions above this 239-ns isomer, starting from the previously known 207- and 655-keV γ rays associated with the isomeric decay [1]. Figure 1(a) presents the result of a double-gate set on these two transitions in the PPP coincidence cube. The 789-keV transition is clearly present in this spectrum together with a weak peak at 1342 keV. Note also two other weak transitions at 1040 and 1222 keV. Accompanying these is a similarly weak (hardly visible in Fig. 1(a)) γ ray at 842 keV. These most likely correspond to neutrons interacting with elements within the detectors (see discussion below).

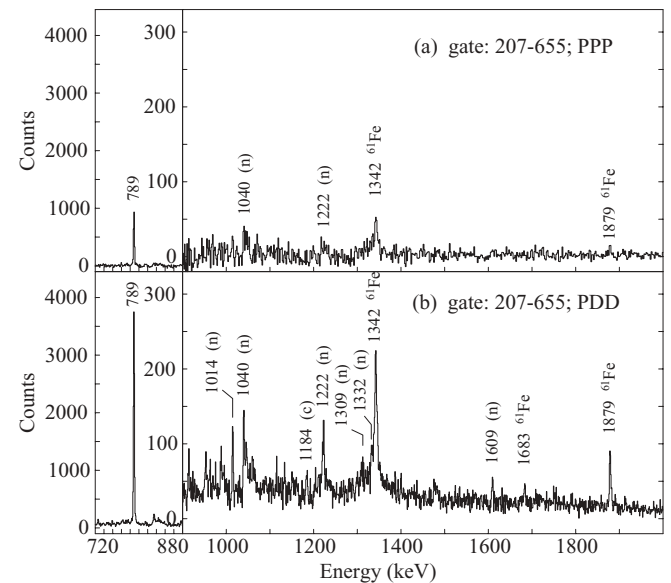


FIG. 1. γ -ray spectra from the 207–655 keV coincidence gate in (a) PPP and (b) PDD cubes. Peaks marked with an n indicate γ rays arising from $(n, n'\gamma)$ reactions with elements in the detectors and auxiliary equipment, and c denotes unresolved contaminant transitions from a nucleus other than ^{61}Fe .

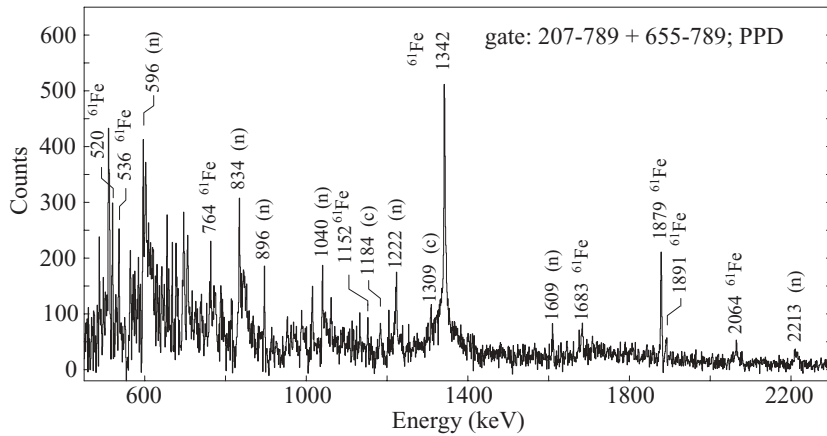


FIG. 2. Spectrum produced from the sum of 207–789 and 655–789 keV coincidence gates in the PPD cube. In the spectrum, *n* denotes peaks that arise from (*n*, *n'*) γ reactions with elements in the detectors and auxiliary equipment and *c* indicates peaks that are associated with unresolved contaminants from a nucleus other than ^{61}Fe .

A similar double-gate on the 207–655 keV γ rays in the PDD cube, displayed in Fig. 1(b), indicates a dramatic enhancement of all the peaks that could be identified in the PPP spectrum, as well as the presence of several new transitions. Most prominent in this spectrum are the peaks at 1014, 1040, 1222, 1342, and 1879 keV, all of which are appreciably weaker than the very intense 789-keV γ ray. As was suggested above, the peaks at 1040 and 1222 keV, and additionally the peak at 1014 keV, can be attributed to neutron-induced reactions with the detector apparatus. In particular, the 1014-, 1040-, and 1222-keV lines are attributed to ^{27}Al , ^{70}Ge , and ^{182}W , respectively. An additional line at 842 keV, which is not readily visible in Figure 1(b), is associated with $^{27}\text{Al}(n, n'\gamma)$. Smaller peaks at 1332 and 1609 keV come from ^{60}Ni and ^{209}Bi , respectively. A complete assessment of neutron-induced reactions in Compton-suppressed Ge detectors has been carried out previously, and can be found in Ref. [17]. Among the transitions that could not be attributed to such reactions are γ rays at 1184, 1309, 1342, 1683, and 1879 keV.

Figure 2 presents the coincidence spectrum resulting from the summation of double gates on the 207–789 and 655–789 keV γ rays. Again, γ rays from neutron-induced reactions are widespread (this is primarily an effect of the location in

energy of the gating transitions). Among the strong lines that could not be attributed to neutrons are 520, 536, 764, 1152, 1184, 1309, 1342, 1683, 1879, 1891, and 2064 keV. Further inspection indicated that the 1342-keV peak is in coincidence with 536-, 1152-, and 1683-keV γ rays. Close scrutiny reveals a possible peak at 1300 keV in the 207–1342 keV double gate, but this transition does not appear above background in the 655–1342 keV double gate. Still, all the gates involving this transition appear to produce consistent results, and the level implied at 4293 keV is supported by a coincidence relationship between the 1879- and 764-keV γ rays. Thus, each of the lines above is placed in the level scheme of Fig. 3, although the assignment of the transition at 1300 keV remains tentative.

The analysis of the γ ray at 1309 keV indicates that it is in coincidence with the 520-keV transition. However, additional coincidence relationships with γ rays at 192, 333, and 369 keV indicate that this cascade belongs to a different nucleus. This leaves the 1184-, 1891-, and 2064-keV lines as the remaining candidate transitions. The 1184-keV γ ray returns 223- and 488-keV lines in coincidence and is, similarly, assumed to belong to a different nucleus. Analyses of the γ rays at 1891 and 2064 keV do not indicate any further coincidence relationships beyond those already established with 207-, 655-,

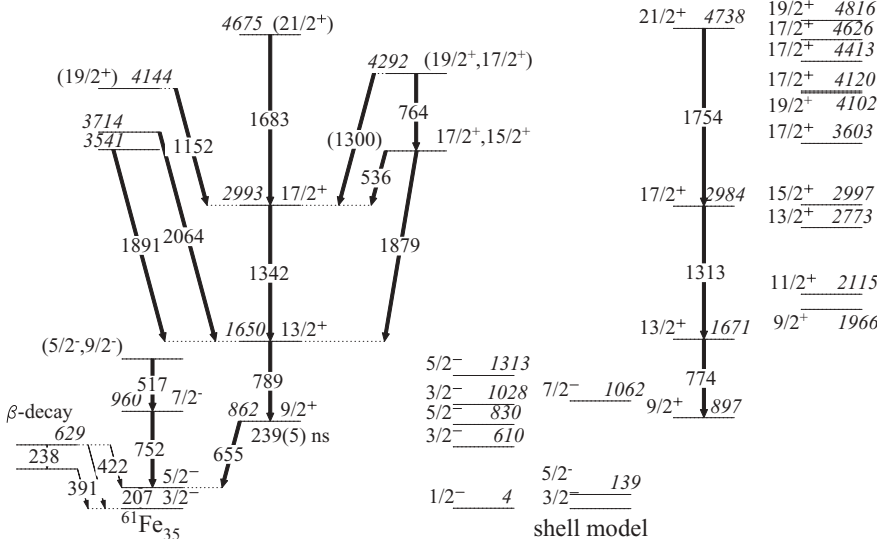


FIG. 3. Level scheme adopted for ^{61}Fe . To the right are the results of shell model calculations described in the text. For simplicity, only calculated yrast and near-yrast levels are given. To the left of the empirical level scheme are two levels and associated γ rays identified from previous β -decay experiments [14], but not in the current work. The arrows linking the calculated levels are present to highlight the agreement between theory and experiment.

and 789-keV transitions. Thus, these lines are included in the level scheme of Fig. 3 directly populating the $13/2^+$ state.

In an independent investigation conducted in parallel with this work, the same reaction was studied but with a thin target and recoil mass gating [18,19]. An additional γ ray at 752 keV was reported in that work, which was found to directly populate the level at 207 keV. Data from the prompt cube in the present experiment clearly support this observation, and an additional transition at 517 keV is also observed to feed this new level.

An angular correlation analysis was performed for the strongest lines that could be identified in the data. As a proof-of-principle, the 655–207 keV sequence, which is known to be of $M2$ - $M1$ character, was analyzed. The resulting a_2 and a_4 angular correlation coefficients are $-0.03(4)$ and $0.07(5)$, respectively, supporting a quadrupole-dipole character in agreement with the literature. In spite of the fact that the 789-keV transition lies above the isomer, its intensity allows a determination of its angular correlation, which is determined from a gate on the 655-keV γ ray to possess a quadrupole character [$a_2 = 0.18(4)$, $a_4 = 0.05(6)$]. Similarly, an analysis of the 1342-keV transition supports a quadrupole character as well [$a_2 = 0.12(11)$, $a_4 = 0.00(16)$], from a gate on the 789-keV γ ray], whereas the 752–207 keV correlation indicates a dipole-dipole cascade ($a_2 = 0.26(4)$, $a_4 = 0.07(6)$).

On the basis of the angular correlation fits described above, the level at 1650 keV is determined to have spin and parity $13/2^+$, consistent with previous suggestions [15]. The most intense transition above the level at 1650 keV is the 1342-keV line of quadrupole character which most likely represents the next excitation of this sequence. Thus, a $17/2^+$ spin and parity are adopted for the state at 2993 keV. Similarly, the level at 4675 keV is tentatively assigned $21/2^+$. From feeding patterns, the sequence of levels at 3529 and 4293 keV could have $J^\pi = 17/2^+$ and $19/2^+$, respectively. These assignments also appear to be supported by the shell model calculations discussed below, but alternative respective assignments of $15/2^+$ and $17/2^+$ cannot be rigorously ruled out.

The level at 960 keV implied by the 752-keV γ ray is assigned a spin of $7/2$ on the basis of its dipole character determined from angular correlations. A negative parity is assigned, primarily from systematics.

TABLE I. Level energies, γ -ray energies, and proposed spin and parity assignments obtained from the present experiment.

E_{level} (keV)	J^π	E_γ (keV)
207	$5/2^-$	207.0(1)
862	$9/2^+$	654.8(1)
960	$7/2^-$	752.5(2)
1477	$(5/2^-, 9/2^-)$	517.1(2)
1650	$13/2^+$	788.5(1)
2993	$17/2^+$	1342.3(3)
3529	$(17/2^+, 15/2^+)$	1878.6(4)
		536.1(3)
3541		1891.1(6)
3714		2064.1(6)
4145	$(19/2^+)$	1151.9(2)
4293	$(19/2^+, 17/2^+)$	763.6(2)
		(1300)
4675	$(21/2^+)$	1682.7(3)

In addition to the levels described above, Fig. 3 shows two additional states at 391 and 629 keV that were previously identified from β decay [14]. Transitions associated with the deexcitation of these levels were not observed in this experiment, most likely because of the low multiplicity of these events. The γ rays, level energies, and proposed spins and parities that were established from this measurement are summarized in Table I.

IV. DISCUSSION

One of the striking features arising from this work is the strong correlation between the first few yrast levels in ^{60}Fe and those of the $9/2^+$ band in ^{61}Fe , as displayed in Fig. 4. The recent measurement of the quadrupole moment of the $9/2^+$ state [5] gives a clear indication that this state is deformed, but the sign of the deformation is not presently known. At face value, the mere fact that the $9/2^+$ state is isomeric would appear to support the contention of an oblate shape, since, in this case, the $9/2[404]$ Nilsson orbital would

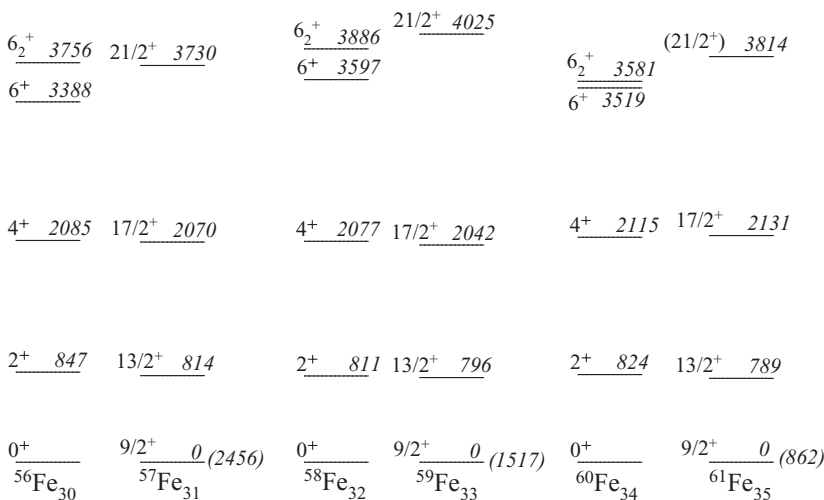


FIG. 4. Yrast levels in even- A Fe isotopes compared with $9/2^+$ band excitations in the associated $A+1$ isotope. For the odd- A isotopes, energies are given relative to the $9/2^+$ state.

be expected to decrease substantially in energy; whereas in the event of prolate deformation, the $1/2[440]$ state would be lowered. In the latter case, the existence of a $1/2^+$ bandhead is clearly not supported by the isomeric character of the $9/2^+$ state. However, according to the model by Stephens [20], at small deformation, a cross-shell excitation could take on a spherical orbit coupled to the rotational motion of a prolate core. This phenomenon, known as rotation-aligned coupling, is traditionally characterized by the parallel band structures exhibited between an odd- A nucleus and its $A-1$ core, similar to that described above. Such an explanation was suggested by Nathan *et al.* [21] to account for a similar trend in $^{56,57}\text{Fe}$. However, a recent analysis of the yrast structure of ^{60}Fe gave no indication of a deformed-rotational structure at low spin in ^{60}Fe [22].

To shed more light on the character of the $9/2^+$ band, shell model calculations were performed within a truncated pf g model space. The residual interaction used for this study was derived from the N3LO bare NN potential using the G -matrix formalism prescribed in Ref. [23]. The interaction assumes an inert ^{48}Ca core, with a model space that includes the $\pi(f_{7/2}, p_{3/2}, p_{1/2}, f_{5/2})$ and $\nu(p_{3/2}, p_{1/2}, f_{5/2}, g_{9/2})$ orbitals. A previous version of this interaction, in which the $g_{9/2}$ neutron orbital was not included, was described in Ref. [9], where results of shell-model calculations were discussed for new levels identified in ^{64}Fe . As in Ref. [9], the single-particle energies used for this study were derived empirically from states outside the double-magic nucleus ^{48}Ca , and these are given in Table II. For the calculations shown in Fig. 3, protons were restricted to the $f_{7/2}$ orbital only, and a maximum of two excitations into the $\nu g_{9/2}$ orbital was allowed.

The model space truncations described above clearly differ from those employed previously by Matea *et al.* [4], who allowed up to 6p-6h excitations. In this work, it is noted that a similar truncation scheme, while giving a similar result for the energy of the $9/2^+$ state, could not reproduce the other levels known in the level scheme. In contrast, the scheme described above, as illustrated in Fig. 3, yields good results for all the levels known in this nucleus. However, the exact agreement

depicted in Fig. 3 was contingent on the lowering of the $\nu g_{9/2}$ single-particle energy, which had the effect of lowering the positive-parity levels relative to the $3/2^-$ ground state. The relative spacing of these levels and the properties of the negative-parity states were unaffected by this lowering. In fact, the reason for doing this was only to emphasize the *relative* agreement of the positive-parity levels with experiment.

Using the wave functions from the calculation detailed above, the intrinsic quadrupole moment was computed to be $Q_0 = +116 e \text{ fm}^2$. This value is in agreement with the recently measured spectroscopic quadrupole moment $Q_s = |42| e \text{ fm}^2$, which, assuming $K = 1/2$, corresponds to $Q_0 = +115 e \text{ fm}^2$. Hence, the shell model calculation appears to support the contention of a prolate shape. Furthermore, this agreement strengthens the argument that the truncations used in the shell model calculation above are, indeed, reasonable. Note that the effective proton and neutron charges used for this calculation were $1.5 e$ and $0.5 e$, respectively, which are consistent with those used in Ref. [4].

In an attempt to view the structure of ^{61}Fe within the scope of a collective model, calculations were performed with the particle-triaxial-rotor (PTR) model. For these calculations, standard parameters κ and μ of the modified oscillator potential were used, as defined in Ref. [24]. Pairing was treated in the standard BCS approximation with parameters $\text{GN}0 = 22.0$ and $\text{GN}1 = 8.0$ [25]. The core nucleus was taken to be ^{60}Fe and both calculated positive- and negative-parity energy levels were in very good agreement with experiment for the value of deformation parameter $\beta_2 \sim 0.23\text{--}0.25$, indicating a similar prolate shape for both the ^{61}Fe ground state and the $9/2^+$ isomer. Details of the calculation will be published elsewhere [26]. Displayed in Fig. 5 are the results of the PTR calculation for electric quadrupole and magnetic dipole moments as a function of deformation parameter β_2 , clearly supporting the deformation derived from the fit to experimental energy levels.

TABLE II. Single-particle energies used in the shell model calculations described in the text.

Orbital	Energy (MeV)
$\pi p_{1/2}$	4.493
$\pi f_{5/2}$	4.072
$\pi p_{3/2}$	3.087
$\pi f_{7/2}$	0.000
$\nu g_{9/2}$	4.072 ^a
$\nu p_{1/2}$	2.023
$\nu f_{5/2}$	3.585
$\nu p_{3/2}$	0.000

^aThe single-particle energy for the $\nu g_{9/2}$ orbital was decreased to 2.372 MeV for the calculation shown in Fig. 3.

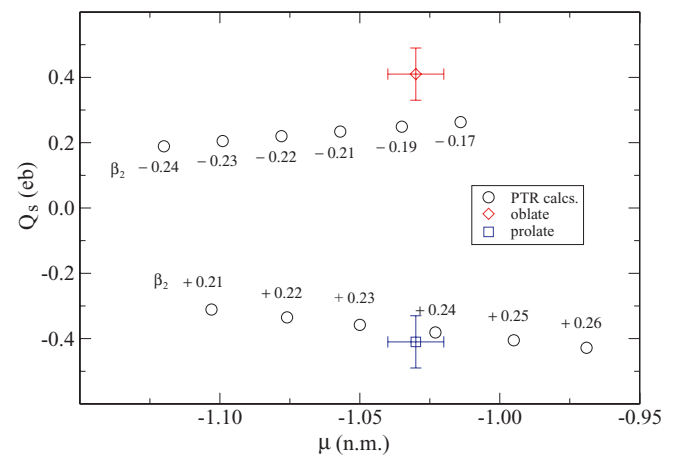


FIG. 5. (Color online) Results from the PTR calculations for the cases of prolate ($K = 1/2$) and oblate ($K = 9/2$) deformation. Calculated data points are labeled with the β_2 deformation used in the calculation. The experimental values are consistent with a prolate deformation of $\beta_2 \sim 0.24$.

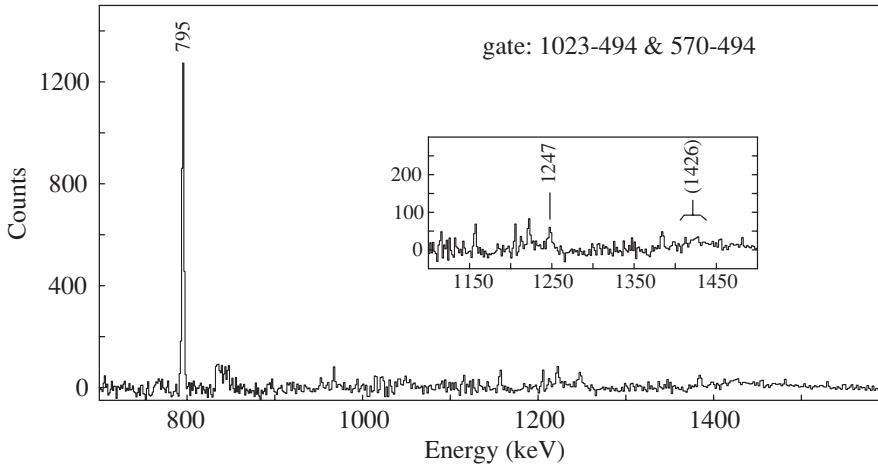


FIG. 6. Spectrum produced for ^{59}Fe based on γ rays reported in Ref. [22]. The main yrast transition at 1426 keV is not observed, since it is associated with a short state lifetime, whereas side feeding via the 1247-keV transition is observed. See text for further discussion.

As a practical measure, it is important to consider the lifetimes of excited states with respect to the stopping time of product nuclides in the target. Of primary concern is whether stretched quadrupole transitions in a prolate band would proceed faster than the time it takes for ^{61}Fe to stop in the target. If this were the case, the transitions would be Doppler broadened sufficiently that it would be impossible to observe them in a thick-target deep-inelastic reaction experiment. Given $Q_0 = +115 e \text{ fm}^2$, one can estimate the mean lifetime of the 1342-keV, $17/2^+ \rightarrow 13/2^+$ transition to be $\tau \approx 0.4 \text{ ps}$, compared to the estimated stopping time of ^{61}Fe in ^{238}U , which is on the order of 1 ps. As the two values are comparable in magnitude, one would expect some degree of broadening in the 1342-keV peak. In fact, some Doppler broadening is evident in the spectra of Figs. 1 and 2, so the contention of a deformed band with stretched quadrupole transitions is not unreasonable. Not only that, but the absence of any transitions beyond $J^\pi = 21/2^+$ might be attributed to the fact that the transition rate increases farther up the band. This point is illustrated further in Fig. 6, which provides the result of a summation of coincidence gates below the $9/2^+$ state in ^{59}Fe . The absence of the known [22] 1426-keV, $17/2^+ \rightarrow 13/2^+$ transition is a clear indication that the lifetime of the $17/2^+$ level must be markedly shorter than the stopping time of ^{59}Fe in ^{238}U . This fact is directly analogous to the broadened 1342-keV peak in ^{61}Fe . In contrast, the 1247-keV, ^{59}Fe γ ray reported as a side-feeding transition in Ref. [22], can be seen in Fig. 6 apparently without any broadening. This could represent a transition analogous to the 1879-keV transition observed in this work.

While a fairly consistent picture appears to emerge from this discussion, it should be acknowledged that a number of issues remain that cannot readily be reconciled with the proposed interpretation. For example, the data on ^{59}Cr [11], the isotone of ^{61}Fe , and on ^{60}Cr [8] have been interpreted in terms of excitations associated with a weakly deformed oblate shape, based on comparisons with TRS calculations. For the ^{61}Fe isotone to be characterized by a prolate shape would presumably require the addition of $f_{7/2}$ protons to be driving the shape toward prolate deformation. If this were the case, however, one would expect these same protons to affect the shape of the ^{60}Fe core in the same way. As

already mentioned above, the level structure of the latter nucleus has recently been significantly expanded [22]. It was shown that shell model calculations are able to reproduce satisfactorily the yrast sequence up to the 10^+ state within the pf model space. Evidence for $g_{9/2}$ excitations is, however, present at higher energies and angular momenta. In Ref. [22], the associated sequences were compared with the results of TRS calculations, which demonstrated that the shape of any particular configuration is greatly influenced by the aligned quasiparticles it contains. In fact, the calculations reflect a situation in which the underlying cores are soft with respect to deformation, and definite conclusions regarding shapes and particle alignments could not be formulated. Rather, more sophisticated calculations were called for. Such, beyond mean field, calculations would also be very useful to clarify the situation in ^{61}Fe .

V. CONCLUSIONS

In conclusion, several new levels have been identified in ^{61}Fe , determined from correlated prompt and delayed coincidence gates following deep-inelastic reactions of ^{64}Ni and ^{238}U . The new levels, as well as some previously known levels are reproduced reasonably well with shell model calculations within a truncated pf model space and additionally with PTR calculations. Both models produce quadrupole moment values that are in good agreement with the measured value from Vermeulen *et al.* [5], although those authors could not determine the sign of deformation. With the current results, a prolate deformation is suggested for the $9/2^+$ isomeric state, and the positive-parity band fits within a rotation-aligned coupling picture, although open questions remain.

ACKNOWLEDGMENTS

This work was supported by the US Department of Energy, Office of Nuclear Physics, under Contracts DEFG02-94ER40834 and DE-AC02-O6CH11357 and by the Polish Scientific Committee Grant 2PO3B-074-18.

- [1] R. Grzywacz, R. Béraud, C. Borcea, A. Emsallem, M. Glogowski, H. Grawe, D. Guillemaud-Mueller, M. Hjorth-Jensen, M. Houry, M. Lewitowicz *et al.*, Phys. Rev. Lett. **81**, 766 (1998).
- [2] M. Hannawald, T. Kautzsch, A. Wöhr, W. B. Walters, K. L. Kratz, V. N. Fedoseyev, V. I. Mishin, W. Böhmer, B. Pfeiffer, V. Sebastian *et al.*, Phys. Rev. Lett. **82**, 1391 (1999).
- [3] O. Sorlin, C. Donzaud, F. Nowacki, J. C. Angélique, F. Azaiez, C. Bourgeois, V. Chisté, Z. Dlouhy, S. Grévy, D. Guillemand-Mueller *et al.*, Eur. Phys. J. A **16**, 55 (2003).
- [4] I. Matea, G. Georgiev, J. M. Daugas, M. Hass, G. Neyens, R. Astarbatyan, L. T. Baby, D. L. Balabanski, G. Bélier, D. Borremans *et al.*, Phys. Rev. Lett. **93**, 142503 (2004).
- [5] N. Vermeulen, S. K. Chamoli, J. M. Daugus, M. Hass, D. L. Balabanski, J. P. Delaroche, F. de Oliveira-Santos, G. Georgiev, M. Girod, G. Goldring *et al.*, Phys. Rev. C **75**, 051302(R) (2007).
- [6] B. A. Brown, Prog. Part. Nucl. Phys. **47**, 517 (2001).
- [7] E. Caurier, F. Nowacki, and A. Poves, Eur. Phys. J. A **15**, 145 (2002).
- [8] S. Zhu, A. N. Deacon, S. J. Freeman, R. V. F. Janssens, B. Fornal, M. Honma, F. R. Xu, R. Broda, I. R. Calderin, M. P. Carpenter *et al.*, Phys. Rev. C **74**, 064315 (2006).
- [9] N. Hoteling, W. B. Walters, R. V. F. Janssens, R. Broda, M. P. Carpenter, B. Fornal, A. A. Hecht, M. Hjorth-Jensen, W. Królas, T. Lauritsen *et al.*, Phys. Rev. C **74**, 064313 (2006).
- [10] A. N. Deacon, S. J. Freeman, R. V. F. Janssens, F. R. Xu, M. P. Carpenter, I. R. Calderin, P. Chowdhury, N. J. Hammond, T. Lauritsen, C. J. Lister *et al.*, Phys. Lett. **B622**, 151 (2005).
- [11] S. J. Freeman, R. V. F. Janssens, B. A. Brown, M. P. Carpenter, S. M. Fischer, N. J. Hammond, M. Honma, T. Lauritsen, C. J. Lister, T. L. Khoo *et al.*, Phys. Rev. C **69**, 064301 (2004).
- [12] R. Broda, J. Phys. G **32**, R151 (2006).
- [13] I. Y. Lee, Nucl. Phys. **A520**, 641c (1990).
- [14] E. Runte, K. I. Gippert, W.-D. Schmidt-Ott, P. Tidemand-Petersson, L. Ziegeler, R. Kirchner, O. Klepper, P. Larsson, E. Roeckl, D. Schardt *et al.*, Nucl. Phys. **A441**, 237 (1985).
- [15] T. Pawlat, R. Broda, B. Fornal, W. Królas, D. Bazzacco, S. Lunardi, C. R. Alvarez, G. de Angelis, G. Maron, D. Napoli *et al.*, LNL Annual Report (1995).
- [16] B. Fornal, IFJ Krakow Annual Report (1994).
- [17] R. Holzmann, I. Ahmad, R. V. F. Janssens, T. L. Khoo, D. C. Radford, M. W. Drigert, and U. Garg, Nucl. Instrum. Methods Phys. Res. A **260**, 153 (1987).
- [18] S. M. Lenzi, S. Lunardi, F. D. Vedova, N. M. Märginean, A. Gadea, E. Farnea, D. R. Napoli, G. de Angelis, D. Bazzacco, S. Beghini *et al.*, Legnaro National Laboratory 2006 Annual Report (2007).
- [19] S. Lunardi, S. M. Lenzi, F. D. Vedova, E. Farnea, A. Gadea, N. Märginean, D. Bazzacco, S. Beghini, P. G. Bizzeti, A. Bizzeti-Sona *et al.*, Phys. Rev. C **76**, 034303 (2007).
- [20] F. S. Stephens, Rev. Mod. Phys. **47**, 43 (1975).
- [21] A. M. Nathan, J. W. Olness, E. K. Warburton, and J. B. McGroarty, Phys. Rev. C **17**, 1008 (1978).
- [22] A. N. Deacon, S. J. Freeman, R. V. F. Janssens, M. Honma, M. P. Carpenter, P. Chowdhury, T. Lauritsen, C. J. Lister, D. Seweryniak, J. F. Smith *et al.*, Phys. Rev. C **76**, 054303 (2007).
- [23] M. Hjorth-Jensen, T. T. S. Kuo, and E. Osnes, Phys. Rep. **261**, 125 (1995).
- [24] T. Bengtsson and I. Ragnarsson, Nucl. Phys. **A436**, 14 (1985).
- [25] I. Ragnarsson and R. K. Sheline, Phys. Scr. **29**, 385 (1984).
- [26] J. R. Stone (to be published).